Species-specific loss of genetic diversity and exposure of deleterious mutations following agricultural intensification

Zachary J. Nolen[1*], Patrycja Jamelska[1,2], Ana Sofia Torres Lara[1,3], Niklas Wahlberg[1], Anna Runemark[1]

[1] Department of Biology, Lund University, Lund, Sweden 22362
[2] Institute of Biology, University of Neuchâtel, Neuchâtel, Switzerland 2000
[3] Faculty 2 Biology/Chemistry, University of Bremen, Bremen, Germany 28359

*Corresponding author: Zachary J. Nolen

Email: zachary.nolen@biol.lu.se

Author Contributions: Zachary J. Nolen: Conceptualization, Methodology, Formal analysis, Investigation (Lead), Data curation, Writing – original draft, Visualization, Funding acquisition. **Patrycja Jamelska**: Investigation (Supporting). **Ana Sofía Torres Lara**: Investigation (Supporting), Writing - review & editing. **Niklas Wahlberg:** Methodology, Writing – review & editing, Supervision. **Anna Runemark:** Conceptualization, Methodology, Writing – review & editing, Supervision, Funding acquisition.

Keywords: Conservation, agricultural intensification, inbreeding, genetic load, genomic erosion

Abstract

Agriculture driven land-use change is a major contributor to insect declines globally. As a result of population decline and subdivision, species lose genetic diversity, potentially reducing adaptive potential and increasing genetic load, reinforcing decline. We examine how genetic diversity has changed over the past century in three Polyommatinae butterfly species in Sweden, leveraging genome sequencing of specimens from museum collections. Based on 63 historical and 92 contemporary genomes, we document a general decline in genetic diversity and reveal that the extent of decline depends on habitat specialization. The habitat generalist has retained most of its genetic diversity and connectivity. In contrast, the two specialists have declined sufficiently that even common variation is being eroded by drift, with up to a 3.3% reduction in heterozygosity per decade in the strongly grassland associated *Cyaniris semiargus*. While this sharp decline has reduced the burden of strongly deleterious mutations in the specialist species, increased population isolation has led to inbreeding in *Cy. semiargus*, exposing a greater proportion of weakly deleterious mutations in homozygous state. This realized burden likely reduces mean fitness and reinforces population decline, highlighting the need for well-connected grassland landscapes to maintain grassland specialist functional connectivity and genetic diversity. We complement these analyses with seven additional Polyommatinae species, uncovering that declines are common across the group, with alarming rates of genetic decline in species listed as viable. This study highlights the urgency of incorporating genetic data into conservation planning, as threats from genetic erosion are not captured by current conservation assessment.

Introduction

Insect decline has received increased attention in recent years as reports uncover alarming declines in insect assemblages and biomass (1). Efforts to quantify this decline estimate that terrestrial insects are declining at an average rate of 11% per decade globally, with this trend being primarily driven by even stronger regional declines in Europe and North America (2). This stark decline is the result of a variety of anthropogenic pressures, primarily climate change and land use changes such as agricultural intensification and urbanization (1, 3–7). Intensive agricultural landscapes place a particularly strong pressure on grassland insect species (6), especially in Europe where formerly biodiverse semi-natural grasslands have been abandoned or converted into intensively cultivated land (8).

While these declines already have alarming implications for natural communities and ecosystem services in which insects play key roles, they can also leave insect populations with genetic challenges to long term persistence. Smaller populations are expected to lose genetic diversity faster than larger populations due to the stronger relative force of drift (9). This reduces their ability to adapt to changing environments (10, 11) and may allow partially recessive, weakly deleterious mutations to accumulate and become unmasked through inbreeding and weakened selection (12, 13). Such accumulation of weakly deleterious mutations increases the genetic load, classically defined as the reduction in population fitness from an optimum genotype (14). This, in turn, may reinforce demographic decline in a process referred to as mutational meltdown (15). An increasing number of studies even document that decline of genetic diversity and accumulation of deleterious mutations may continue after demographic recovery due to drift debt (16–19).

How to assess the threat genetic factors pose to natural populations is still an active area of research, with several genetic monitoring approaches being suggested and implemented (20–23). Interpretation of genetic diversity is complex, as it is influenced by a multitude of factors (24), such as ecology and life history (25), genomic architecture (26), and demographic trends over thousands to millions of years (27). Some empirical studies

have shown that populations may persist despite low levels of genetic diversity (28, 29) and that relationships between genetic diversity and extinction risk are context dependent (30). Therefore the value of neutral genetic diversity in conservation management has been subject to some debate (31–33).

As a means to control for factors that may make interpreting absolute estimates of genetic diversity challenging, measures that estimate the rate of genetic erosion have seen increasing focus in genetic monitoring. Programs in several countries use genetic metrics measured at multiple time points or that directly estimate ongoing genetic decline (21, 34, 35). Examining decline directly rather than setting thresholds for absolute levels of genetic diversity enables identifying populations for which 'low' genetic diversity is likely to increase extinction risk. For instance, larger populations are expected to have higher numbers of segregating deleterious mutations (36), making them more prone to inbreeding depression following population decline (12, 37, 38).

Temporal sampling is, however, limited to estimating genetic decline from the first sampled time point, with considerable erosion likely to have occurred several decades before. To overcome this, genomic resources from historic samples preserved in natural history museums can extend monitoring further back in time. The direct measures of pre- and early bottleneck genetic parameters museum samples provide are crucial to fully understand the extent and character of genetic decline (23). Comparisons with historical samples may even allow approximating changes in genetic load across bottlenecks by comparing counts of putatively deleterious mutations (12, 19, 23, 39–41). Such studies have the potential to identify populations that face reduced fitness from decline.

Here, we use museomics to address to what extent genetic diversity has been lost and functional connectivity reduced in grassland associated butterflies during the second wave of agricultural modernization in Sweden starting in the 1940s (42, 43). During this modernization, small farms were abandoned, and their associated semi-natural grasslands began to decline considerably (43). We examine three focal butterfly species in this landscape that vary in habitat specialization, ranging from grassland generalist to

specialist, enabling us to examine if patterns of genetic decline are stronger in more specialized species, in line with expectations from greater demographic declines in specialist insect abundance compared to generalists (44–46). By comparing pairs of historical population samples collected in southern Sweden in the early 20th century with their contemporary counterparts, we document species-specific losses of genetic diversity and functional connectivity, and increased homozygosity of putatively deleterious mutations that is expected to have increased genetic load in the most specialized species. We further examine if patterns of loss of genetic diversity are general, and if loss of genetic diversity is reflected in current conservation status, by extending the dataset to include historical and modern individuals of seven additional related butterfly species with Swedish Red List (47) conservation statuses ranging from least concern to critically endangered.

Results

We analyzed changes in genetic diversity, differentiation, and deleterious mutation burden in three focal Polyommatinae (Lepidoptera: Lycaenidae) butterfly species: *Polyommatus icarus,* a grassland generalist, *Plebejus argus*, a heathland specialist, and *Cyaniris semiargus*, a grassland specialist (Figure 1A). We generated whole genome resequencing data from pinned museum specimens from the entomological collections of the Biological Museum at Lund University (48) collected from 1917-1956 (Table S1; *N* = 28 - *Po. icarus*; 12 - *Pl. argus*; 14 - *Cy. semiargus*) in southern Sweden. These individuals were sampled in populations generally collected at the same locality during the same year, and compared with WGS data from samples collected at corresponding localities in 2020-2023 by Nolen et al (49) (Figure 1B; Table S1; *N* = 27 - *Po. icarus*; 29 - *Pl. argus*; 29 - *Cy. semiargus*). As DNA extracted from historical specimens is fragmented and subject to post-mortem DNA damage (50, 51) (Figure S1), we confirmed shorter fragments did not induce a reference bias in the historical samples (Figure S2). To address DNA damage, we tested post-mortem DNA damage correction I) using MapDamage2 (52) and II) removing all transition sites, which are the most common changes caused by DNA damage (50, 51). Rescaling base quality scores with MapDamage2 biased historical samples towards the reference in

two of the three focal species, whereas transition removal did not (Figure S2). All subsequent results were therefore generated without MapDamage2 correction and with transitions removed. To account for lower sequencing depth in historical samples, we performed analyses both at full depth and with samples subsampled to equivalent mean sequencing depths, presenting the subsampled results in the main text, with full depth results included in the Appendix.

General reductions in genetic diversity

To assess if agricultural intensification and the associated reduction in semi-natural grassland habitat has resulted in reduced genetic diversity, we compared individual genome-wide heterozygosity of historical and modern samples within each species. In all three species, heterozygosity is lower in modern individuals, but considerably more so in the two specialist species compared to the generalist (Welch two-sample t-test: $P = 0.006$ in *Po. icarus*, < 0.001 in *Pl. argus*, and < 0.001 in *Cy. semiargus;* Figure 1C; Tables S2-3). In the specialist species, *Pl. argus* and *Cy. semiargus*, population-specific estimates of genetic diversity are lower in all modern populations compared to their historical counterparts, both for nucleotide diversity (π; Wilcoxon signed-rank test: median effect size range [-0.52, -0.40] in *Pl. argus* and [-0.76, -0.51] in *Cy. semiargus*) and Watterson's θ (median effect size range [-0.77, -0.68] in *Pl. argus* and [-0.86, -0.70] in *Cy. semiargus*), even after subsampling to account for variation in sample size (Figure S3; Tables S4-5). In the generalist, *Po. icarus*, only Watterson's θ shows declines robust to variation in sample size, and only in two of the three populations (median effect size range [-0.29, -0.24]; Figure S3; Table S4-5). Tajima's D is higher in modern populations of all three species compared to their historical counterparts, consistent with population bottlenecks across the past century (median effect size range [0.63, 0.68] in *Po. icarus*, [0.82, 0.84] in *Pl. argus*, and [0.73, 0.85] in *Cy. semiargus*; Figure S3; Table S4-5).

Reduced connectivity may accelerate loss of genetic diversity

While genetic diversity decline is an expected product of demographic decline, it can additionally be accelerated by reductions in gene flow (53). We reveal a loss of functional

connectivity among modern populations, reflected in the stronger contemporary population structure uncovered by both genetic differentiation and clustering approaches, likely contributing to the loss of genetic diversity. *Po. icarus* and *Cy. semiargus* have stronger genetic differentiation (F_{ST}) between modern than historical population pairs (Paired t-test: ΔF_{ST} = 0.014, P = 0.007 in *Po. icarus* and ΔF_{ST} = 0.053, P = 0.036 in *Cy. semiargus*; Figure 1F; Table 6-7). F_{ST} increased in *Pl. argus* in the single population pair present in both time periods (ΔF_{ST} = 0.021; Table S7). Including all modern population pairs in the analysis estimates mean F_{ST} increases of 0.027 and 0.071 in *Pl. argus* and *Cy. semiargus*, respectively (Welch two-sample t-test: P = 0.001 in *Cy. semiargus*; Table S7). Principal component analyses (PCAs) and admixture analyses also reveal generally stronger population structure in modern samples than historical, and strongest in the most specialized *Cy. semiargus* (Figure 2A). Along PC1, the greatest axis of variation, both *Po. icarus* and *Pl. argus* are clustered primarily into historical and modern samples, consistent with the best fit admixture analyses for these species (K=2; Figure 2B; Table S8). In these two species, modern samples show greater among population differences than historical along PC2, however, consistent with increases in genetic differentiation between localities. However, more than two clusters are visible on the PCA for these two species, supported by the correlation of residuals for the admixture analyses (Figure S4). This highlights that greater genetic structure likely exists in these two species, but described by too little variation to reliably cluster samples by at these sample sizes. Each modern population forms a distinct cluster in the specialized species, *Cy. semiargus*, while historical populations cluster together in a single separate cluster (Figure 2B). The stronger contemporary population structure is especially driven by isolation of populations in the agricultural landscapes within Sweden's southernmost province, Skåne (Figure 1D; Figure 2B; Figure S5).

Species-specific increases in inbreeding

The pronounced losses of functional connectivity and genetic diversity have resulted in inbreeding within the specialist *Cy. semiargus*. This contemporary inbreeding is reflected by an increase in the inbreeding coefficient F_{RoH} from historical to modern *Cy. semiargus*

177 samples (Welch two-sample t-test: ΔF_{RoH} = 0.065, P < 0.001; Figure 1D; Table S3&9). F_{RoH}
178 measures the proportion of the autosomal genome in runs of homozygosity greater than a
179 certain length (54), which we set to 100kb, roughly corresponding to identical by descent
180 tracts with shared ancestry in the past 200 generations (55). Across species, no historical
181 individual has a coefficient greater than 0.04, and historical species averages are all below
182 0.01. In *Cy. semiargus*, modern samples have a maximum coefficient of 0.33 and an
183 average coefficient of 0.072, an order of magnitude higher than the mean for historical
184 samples. In modern *Cy. semiargus*, individuals with higher inbreeding coefficients have
185 fewer runs of homozygosity relative to their cumulative length, which may indicate they
186 stem from close-kin matings (Figure 3A, Figure S6). For other individuals, there is a largely
187 linear relationship between the number of runs of homozygosity and their cumulative
188 length, suggesting that close-kin mating is not common overall and inbreeding is primarily
189 due to increases in background relatedness, consistent with patterns expected of a
190 population bottleneck (55).

191 Purging of deleterious mutation burden

192 Population decline and subdivision can increase the exposure of partially recessive,
193 deleterious mutations to selection due to increased homozygosity, facilitating purging of
194 strongly deleterious mutations (56–58). However, as populations decline and subdivide,
195 selection weakens relative to drift, allowing partially recessive, weakly deleterious
196 mutations to drift to higher frequencies and fix, increasing genetic load (13, 15, 59). Here,
197 we estimated deleterious mutation burden using relative counts of putatively deleterious
198 mutations per individual as a proxy for genetic load (as in e.g. 19, 39, 41, 60, 61). We
199 separate putatively deleterious mutations into three groups. Weakly deleterious include
200 missense mutations, strongly deleterious consist of e.g. loss of function mutations, and
201 highly conserved include derived mutations at positions with high sequence conservation
202 in Lepidoptera, presumed to be strongly deleterious. We find evidence consistent with
203 purging of deleterious mutations in both specialist species *Pl. argus* and *Cy. semiargus*,
204 with the relative count of strongly deleterious mutations being lower in modern compared
205 to historical individuals in both species (Welch two-sample t-test: P = 0.018 in *Pl. argus*

206 and 0.031 in *Cy. semiargus*; Figure 3B; Table S10). Burden from weakly deleterious
207 mutations has also decreased somewhat in *Pl. argus* ($P < 0.001$; Figure 3B; Table S10). In
208 generalist *Po. icarus*, burden from weakly and strongly deleterious mutations is similar in
209 modern and historical samples. Burden from derived alleles at highly conserved positions
210 positions has remained stable in all three species (Figure 3B; Table S10).

211 Increased homozygosity of weakly deleterious burden in *Cy. semiargus*

212 Weakly deleterious mutations are exposed in a homozygous state more often in modern
213 than historical *Cy. semiargus* individuals ($P < 0.001$; Figure 3C; Table S10). In contrast,
214 strongly deleterious mutations are homozygous at equal rates over time. In *Po. icarus* and
215 *Pl. argus*, we find no evidence for increases in homozygosity of weakly or strongly
216 deleterious mutations (Figure 3C; Table S10). However, derived variants at conserved
217 regions are homozygous to a greater extent in modern samples of both *Pl. argus* and *Cy.*
218 *semiargus* ($P < 0.001$ in *Pl. argus* and = 0.009 in *Cy. semiargus*; Figure 3C; Table S10). In *Cy.*
219 *semiargus*, individuals with higher inbreeding coefficients had higher homozygous, but not
220 total, deleterious burden across all categories of deleterious mutations (linear regression:
221 R^2 = 0.79, 0.18, 0.35 for weakly, strongly, and conserved deleterious variants, respectively;
222 Figure S7). This suggests that increased rates of inbreeding have increased homozygosity
223 of deleterious mutations, and that this effect is strongest for weakly deleterious mutations.

224 Genetic decline not reflected in current conservation status

225 We utilized the genetic decline indicator thresholds outlined by Andersson et al. (20) to
226 determine if current conservation status relates to the rate of genetic decline. These
227 thresholds suggest categorizations of 'Acceptable', 'Warning', and 'Alarm' rates of genetic
228 decline, reflecting >=95%, 75-94%, and <75% retention of genetic diversity over 100 years,
229 respectively. Based on changes in heterozygosity, nucleotide diversity, and Watterson's θ,
230 *Po. icarus* largely exhibits 'Acceptable' or 'Warning' declines, while *Pl. argus* and *Cy.*
231 *semiargus* exhibit 'Warning' or 'Alarm' declines, depending on the metric of genetic
232 diversity used (Figure 4&S8; Tables S5&11), which largely are in line with the concerns
233 raised by our deleterious mutation burden analyses. This is in stark contrast with the 2020

234 Swedish Red List of species (47), where all three focal species share a conservation status
235 of 'Least Concern'.

236 To assess if the loss of genetic diversity in the three focal species is representative of other
237 grassland butterfly species, we supplemented the dataset by generating whole genome
238 resequencing data for historical-modern pairs of seven additional species of
239 Polyommatinae butterfly (Table S1). We assessed if the conservation status of these
240 species, ranging from of 'Least Concern' to 'Critically Endangered' (47) (Table S12) capture
241 losses of genetic diversity uncovered in this data set. Comparing individual heterozygosity,
242 we find that current conservation status generally fails to capture the levels of genetic
243 erosion in these species (Figure 4A&S8; Table S11). Utilizing estimates at full individual
244 sequencing depth, least concern species predominantly fell into the warning category,
245 with only *Celastrina argiolus* and Öland *Po. icarus* falling in the acceptable category. Of
246 species classified as least concern, only *Cy. semiargus* fell into the alarm category. Two
247 endangered species, *Phengaris alcon* and *Scolitantides orion,* fell into the acceptable and
248 alarm categories, respectively, with *Ph. alcon* even increasing slightly in genetic diversity
249 over the time frame. *Plebejus argyrognomon*, a critically endangered species that is now
250 presumed extinct in Sweden (62), had already experienced genetic decline categorized as
251 'alarm' by the early 2000s, when our modern sample for this species was collected.
252 Results from our focal species illustrate that categorization can depend considerably on
253 the individuals/populations sampled (Figure 4). Categorization is largely consistent for
254 each species both at full sequencing depth and when subsampled to 2-3X sequencing
255 depth, but some species/populations bordering adjacent categories shift between them
256 upon subsampling (Table S11).

257 Discussion

258 Our analyses of 63 historical and 92 modern genomes uncover a decline in butterfly
259 genetic diversity over the past century. This decline is greater in the specialist species,
260 especially *Cy. semiargus*, where the once highly connected populations have become
261 isolated into distinct genetic clusters. This isolation and resulting decline in genetic

262 diversity has resulted in purging of highly deleterious burden in the two specialist species,
263 and even of weakly deleterious burden in *Pl. argus*, which showed intermediate decline.
264 However, in *Cy. semiargus*, where decline was greatest, homozygosity of weakly
265 deleterious burden has increased following inbreeding, most likely resulting in reduced
266 fitness for more inbred populations. The rates of decline uncovered in the three focal
267 species are also common in seven additional species of blue butterflies, despite most of
268 these species having conservation statuses of 'Least Concern'. Our findings reveal that
269 recent genetic erosion is likely to be ubiquitous across grassland butterflies in southern
270 Sweden. These results highlight the need for incorporation of genetic data into
271 conservation assessments of insect threat status, as census-based estimates fail to
272 detect threats posed by genetic decline.

273 Our findings of reduced genetic diversity across all three focal species are consistent with
274 widespread demographic decline in arthropod species in Europe over the past century,
275 with the modernization of agriculture as a major driver (5, 63). The highest average decline
276 in genetic diversity we document, an up to 3.3% reduction in heterozygosity per decade in
277 *Cy. semiargus,* appears to be accelerated by strengthened isolation between populations.
278 However, both *Po. icarus* and *Pl. argus*, where increases in population subdivision are
279 more moderate, have experienced declines of up to 0.7% and 2.7% per decade,
280 respectively. Population structure and genetic differentiation analyses suggest modest
281 increases in population isolation in these species, potentially reflecting that declines in
282 genetic diversity predate genomic signals of population subdivision. Population
283 differentiation accumulates over time, lagging behind barriers to gene flow (64, 65), with
284 the rate at which genetic differentiation accumulates after subdivision depending upon the
285 underlying effective population sizes of the populations (66).

286 Importantly, the finding that these three species have historically had low levels of genetic
287 differentiation across southern Sweden highlights that currently isolated populations may
288 be made up of partitions of historically well-connected metapopulations. Hence, concerns
289 about genetic rescue (67) wiping out locally adapted ancestry (68, 69) are not likely to be
290 relevant for these and other grassland associated insects in regions with historically

291 abundant habitat. Instead, restoring functional connectivity to reduce inbreeding and
292 associated accumulation of deleterious mutations (15, 70) is likely key to improve
293 prospects of long-term persistence. Previous work on *Cy. semiargus* has shown that the
294 inbreeding in these modern populations is related to low grassland land cover in the
295 surrounding landscape (49). Expanding green infrastructure and restoration of semi-
296 natural grassland habitat, enabling dispersal and buffering genetic decline, is likely needed
297 to remedy future isolation and inbreeding in grassland associated butterflies.

298 Understanding to what extent genetic diversity decline, resulting from habitat loss and
299 isolation, reduces the fitness of individuals and populations is crucial for determining
300 conservation priorities. To approximate such genetic load without direct fitness estimates,
301 we quantified deleterious mutation burden (71). Strongly deleterious mutation burden is
302 lower in modern individuals compared to historical for both specialist species. This is in
303 line with theoretical predictions (56–58) and empirical evidence (19, 60, 72–75) suggesting
304 that population decline can increase exposure of partially recessive, strongly deleterious
305 mutations to selection, reducing their frequency. Interestingly, weakly deleterious
306 mutation burden appears to have also decreased in *Pl. argus*, though only mildly (5%
307 reduction compared to 15.7% for strongly deleterious). Weakly deleterious mutations are
308 less likely to be efficiently purged in small populations than strongly deleterious ones (56,
309 58), often requiring low dominance coefficients for purging to be effective (56). Dominance
310 coefficients are generally lower for more deleterious segregating mutations (76), and
311 estimates for the mean dominance coefficients for weakly deleterious mutations are
312 around 0.2-0.25 (77, 78). Despite this, purging of the portion of weakly deleterious burden
313 with high recessivity has been described in the Iberian Lynx, largely occurring at
314 intermediate points of decline before populations were very small (60). Our findings of
315 reduced weakly deleterious burden in *Pl. argus*, which has declined intermediately to the
316 other two species, could partially be explained by purging of only the highly recessive
317 portion of burden, as predicted from models of deleterious mutation count during a
318 bottleneck (60).

319 Considering the partial recessivity of segregating deleterious mutations (77–79) and the
320 frequency of inbreeding depression in outcrossing organisms (59, 68, 80, 81), negative
321 fitness effects for deleterious mutations should be primarily realized when exposed in
322 homozygous state. Genetic load, in turn, is likely more closely approximated by the
323 homozygous rather than total deleterious burden. In the grassland specialist *Cy.*
324 *semiargus*, burden has increased in homozygosity at both conserved positions and for
325 weakly deleterious mutations. As weakly deleterious burden is strongly associated with
326 inbreeding coefficient, this can be interpreted as unmasking of the inbreeding load present
327 in the historical populations (12, 68, 82). Contemporary heterozygosity in *Cy. semiargus*
328 has a strong negative relationship to rates of inbreeding (49). A recent study associating
329 extinction risk with heterozygosity in the Glanville fritillary butterfly (*Melitaea cinxia*) found
330 that for small, isolated, recently declined populations, heterozygosity was negatively
331 associated with extinction and mortality (30). Increased homozygous deleterious mutation
332 burden as we observe in small, isolated, recently declined populations of *Cy. semiargus* is
333 likely what causes the fitness consequences observed in isolated *M. cinxia* populations
334 (30, 83, 84). Joint estimation of fitness and deleterious mutation burden is key to fully
335 understanding how well different measures of mutation burden approximate genetic load.
336 This information is necessary for using genomics based approximations of load to assess
337 conservation status of wild populations.

338 Furthermore, understanding the link between measures of deleterious mutation burden
339 and fitness-based estimates of load is important for assessing the validity of assumptions
340 underlying estimates of burden. For instance, the functional effect based estimates used
341 to classify weakly and strongly deleterious mutations are reliant upon the accuracy of
342 underlying gene models and, in our case, assume the reference allele is less deleterious
343 than the alternate. Estimates of burden using sequence conservation scores also assume
344 more conserved regions are more functionally important (12, 85). Our findings for
345 conserved sites more closely resemble those of weakly deleterious mutations, potentially
346 reflecting the limited ability of sequence conservation scores to distinguish between
347 weakly and strongly deleterious mutations (86, 87). In addition, GERP scores depend on

348 estimates of the rate of neutral evolution, approximating the rejected substitution rate. Our
349 GERP scores are based on a time tree (similar to 39, 40, 74, 86) and hence differ from
350 scores estimated based on neutral rates (e.g. 88). However, our identification of conserved
351 sites should be robust for within-species comparisons of deleterious burden, as they
352 represent the upper extreme of the distribution in our data. Despite these caveats, our
353 estimates of deleterious burden are consistent with expectations under the species-
354 specific patterns of genetic decline, underscoring their relevance to conservation. The
355 strong general pattern of increased deleterious burden expressed in a homozygous state
356 uncovers a potentially serious threat to *Cy. semiargus*. While we uncover fixation of
357 deleterious mutations within populations, almost none are fixed across all populations.
358 This calls for assisted migration and establishment of migration corridors to avoid local
359 mutational meltdown and extirpation in *Cy. semiargus*.

360 None of the three focal species are currently demographically declining at a rate to qualify
361 for the Swedish Red List based on demographic data. Systematic monitoring in Sweden
362 from 2010-2023 reveal declines in both *Po. icarus* and *Cy. semiargus*, while *Pl. argus*
363 appears to have stabilized (89). Demographic stability in *Pl. argus* does not necessarily
364 mean that genetic diversity has stabilized in the species, as populations may continue to
365 lose genetic diversity even after demographic recovery, a phenomenon termed drift debt
366 (16). In *Cy. semiargus*, genetic factors are likely already contributing to its demographic
367 decline. Our findings illustrate the importance of incorporating genetic monitoring into
368 conservation assessment (90, 91) to identify genetic decline before it results in expressed
369 genetic load. Temporal monitoring with historical samples provides an opportunity to
370 detect species facing recent declines in genetic diversity, separating them from those with
371 longer term low genetic diversity (23). Using this approach on several species of
372 Polyommatinae blues in southern Sweden, we document a general loss of genetic diversity
373 in grassland butterflies and uncover that additional species currently not on the Red List
374 likely face threats from reduced genetic diversity. Estimations of genetic decline along with
375 complementary estimates of deleterious burden provide a promising way to assess
376 genetic conservation concerns in the wild (19), but these analyses are limited by the

377 availability of high quality reference genomes. This underscores the importance of efforts
378 to generate high quality references for wild species to improve our ability to accurately
379 assess these metrics (92).

380 In conclusion, we document a general decline in genetic diversity in grassland butterflies in
381 southern Sweden, which is likely mirrored in other regions that have lost grasslands to
382 intensive agriculture and forestry. While demographic declines largely inform current
383 conservation status of these species, we show that this is insufficient to capture declines
384 in genetic diversity and resulting inbreeding, highlighting the acute need for genetic
385 monitoring of wild insects to prevent extirpation and extinction. *Cyaniris semiargus*, a once
386 widespread species in Sweden, provides a strong example of this, now persisting in
387 segmented populations with increased rates of inbreeding and expression of deleterious
388 burden, requiring prompt conservation action to reduce the risk of local extinction.

389 Methods

390 Study System and Sampling

391 To assess changes in genetic diversity, differentiation, inbreeding, and deleterious burden,
392 we selected three blue butterfly species (Polyommatinae) as focal species, *Polyommatus*
393 *icarus*, *Plebejus argus*, and *Cyaniris semiargus* (Figure 1A). These three species were
394 selected as they vary in habitat specialization, being grassland generalist, heathland
395 specialist, and grassland specialist, respectively, in order to assess how specialization
396 may impact genetic decline. For these three species, we used population-level genetic
397 data we previously generated (49) as our modern dataset. We selected pinned specimens
398 from the entomological collections of the Biological Museum, Lund University (48) that
399 corresponded to roughly the same geographic area as the modern samples for each
400 species. These historical specimens were sampled between 1917-1956, during the early
401 stages of the second wave of agricultural modernization in Sweden (42). For each historical
402 locality, we selected 4-11 specimens sampled in the same year to estimate population-
403 level metrics. The historical and modern population-level pairs were sampled in four broad
404 geographic areas: I) Western and II) Eastern Skåne, III) Småland, and IV) Öland (Figure 1B),

405 with historical localities ranging approximately 12-40km from their modern counterparts.
406 This resulted in historical-modern population-level pairs for three regions in *Po. icarus*
407 (Western and Eastern Skåne and Öland), two regions in *Pl. argus* (Småland and Öland), and
408 three regions in *Cy. semiargus* (Western and Eastern Skåne and Småland). While most
409 regions consist of only one historical-modern population pair, we additionally compared a
410 modern *Cy. semiargus* population in Southeastern Skåne to the historical Eastern Skåne
411 population. We were unable to sample population-level historical data for *Pl. argus* in
412 Skåne, however we did sample one historical specimen each from Western and Eastern
413 Skåne, which we include in individual level analyses, pairing them with the modern
414 samples from Southwestern and Eastern Skåne, respectively.

415 To more broadly assess the variation in rates of genetic decline in Polyommatinae of
416 differing conservation statuses, we sampled historical and modern individuals of seven
417 additional species: *Agriades optilete, Aricia agestis, Celastrina argiolus, Polyommatus*
418 *amandus, Phengaris alcon, Scolitantides orion,* and *Plebejus argyrognomon*. Modern
419 specimens of *Ag. optilete, Ar. agestis, Ce. argiolus,* and *Po. amandus* were collected
420 across the same geographic regions as the focal species in 2021 (Table S1). Pinned
421 specimens to be used as modern samples of *Ph. alcon* and *S. orion,* collected in 2003 in
422 Western Skåne and 2016 in Södermanland, respectively, were donated to this study by
423 Håkan Elmqvist. Legs from a pinned speciemen of *Pl. argyrognomon*, collected in 2003 in
424 Western Skåne, were donated by Göran Engqvist and used as the modern sample for this
425 species. The historical samples for these eight species all were selected to be proximal to
426 the modern specimen sampling locality with collection dates ranging from 1932-1967, all
427 provided as pinned specimens from the entomological collections of the Biological
428 Museum, Lund University (48).

429 DNA Extraction and Sequencing

430 DNA from fresh specimens was extracted and sequenced following the methods in Nolen
431 et al (49). We extracted DNA and prepared sequencing libraries from pinned museum
432 specimens in a facility dedicated to historical DNA processing at Lund University, following

433 the protocol described by Twort et al (93). Libraries prepared for pinned specimens were
434 pooled into two equimolar pools containing 37-38 libraries each, sequencing each pool on
435 a single NovaSeq 6000 S4 lane. DNA was extracted from the abdomens or legs of male
436 specimens without homogenization to preserve anatomical structures. Abdomens were
437 then stored in glycerol together with the original specimen.

438 Genomic Analyses

439 We performed the majority of our analyses using the PopGLen pipeline v0.3.0 (94), a
440 Snakemake (95) pipeline we have built that combines several genotype likelihood based
441 population genomic analyses. Genotype likelihood based analyses use a probabilistic
442 framework to account for the uncertainty that comes with low coverage sequencing data,
443 reducing biases related to lower sequencing depth in our historical samples. We utilized
444 genotype likelihood based analyses for all results, except for the estimation of inbreeding
445 coefficients and genetic load, where the chosen methods required called genotypes.

446 *Sequence Processing*

447 We trimmed both modern and historical raw sequencing data using fastp v0.23.4 (96) with
448 default settings, additionally collapsing overlapping read pairs in historical samples,
449 discarding those with less than 30bp overlap. This processing of historical samples
450 discards short (<30bp) fragments that contain little data usable for unique mapping, as
451 well as long fragments (>270bp) that are more likely to be modern contaminants.

452 We mapped the trimmed, paired modern reads separately per sequencing run to the
453 respective species-specific reference genomes, or to the closest relative with an available
454 chromosome-level assembly (Table S12), using BWA mem v0.7.17 (97). We mapped the
455 collapsed historical reads to the same reference genomes using BWA aln, which is the
456 recommended algorithm for reads shorter than 70bp (98) using settings optimized for
457 ancient/historical DNA (`-l 16500 -n 0.01 -o 2`) (99).

458 We merged mapped sequencing runs per sample using Samtools v1.17 (100) and removed
459 PCR and optical duplicates using Picard v2.27 (101) with default settings except for an

460 optical duplicate pixel distance of 2500, as recommended for patterned flow cell data. We
461 removed PCR duplicates for our historical samples using dedup v0.12.8 (102), which
462 identifies duplicates using both ends of the collapsed sequencing read.

463 We realigned around indels using the GATK IndelRealigner (103). As the primary tool we are
464 using, ANGSD (104), counts overlapping reads twice (105), we additionally clipped
465 overlapping read pairs in the modern samples using BamUtil v1.0.15 (106). We estimated
466 post-mortem DNA damage in historical samples using DamageProfiler v1.1 (107).

467 *Site and read filtering*

468 We utilized a site based filtering scheme similar to that implemented by Pečnerová et al
469 (108) in which we developed multiple independent sets of filtered sites, which we
470 intersected to create a global list of filtered sites for all analyses. We performed this
471 filtering for each species dataset separately.

472 We excluded sex-linked chromosomes, mitochondria, and scaffolds less than 1 Mb in
473 length. We excluded repeats identified by RepeatMasker v4.1.2 (109), using the reference
474 specific repeat libraries provided by the Darwin Tree of Life Project
475 (https://projects.ensembl.org/darwin-tree-of-life/). We estimated regions in the lower 1%
476 and upper 99% of global sequencing depth distribution separately across all samples,
477 historical samples, and modern samples, excluding sites that appeared in any of the three
478 sets. The number and proportion of sites passing each of these filters, as well as passing
479 the final intersected filter set, are reported for each species in Table S13. We estimated
480 mean sequencing depth without filtering, as well as within the filtered site set, for each
481 sample using ANGSD (Table S1). All subsequent analyses were performed on the species-
482 specific filtered site sets.

483 *Reference bias and post-mortem DNA damage*

484 We investigated two potential methods to account for post-mortem DNA damage: I)
485 recalibration of putatively damaged bases using MapDamage2 (52), and II) removal of
486 transitions, where most DNA damage is expected to occur (50, 51). We assessed their
487 performance by comparing identity by state (IBS) similarity to the reference at filtered sites

488 between the two correction methods and the uncorrected data (Figure S2). We estimated
489 IBS similarity to the reference for each sample using ANGSD, sampling a single base at
490 each position (`-doIBS 1`), counting reference bases as 1 and non-reference bases as 0 (-
491 `doMajorMinor 4 -output01 1`). We calculated the average IBS similarity per individual
492 from these values, with 1 indicating complete similarity to the reference and 0 indicating
493 complete dissimilarity.

494 Historical samples without correction had less similarity to the reference than modern
495 (Figure S2), as expected for historical samples without substantial mapping bias due to
496 drift from the sampling time of the historical samples and the modern reference as well as
497 differences introduced by post-mortem DNA damage (41, 110). After MapDamage2
498 rescaling, historical samples showed higher similarity to the reference than modern
499 samples in *Po. icarus* and *Pl. argus*. As transition removal did not introduce this reference
500 bias, we proceeded using transition removal in all analyses.

501 *Genotype Likelihood Calculations*

502 We estimated genotype likelihoods in ANGSD v0.940 (104) using the GATK model (`-GL 2`),
503 using reads with a mapping quality greater than 30 (`-mapMapQ 30`) and base quality greater
504 than 20 (`-minQ 20`). We filtered our analyses to sites present in the species-specific filtered
505 sites list using the `-sites` option.

506 *Heterozygosity and genetic diversity metrics*

507 We estimated individual genome-wide heterozygosity for all samples using the single
508 sample site frequency spectrum (SFS) produced by realSFS, included with ANGSD. First,
509 we generated a sample allele frequency (SAF) file (`-doSaf 1`) for each sample, setting the
510 ancestral state (`-anc`) to the reference sequence. We generated a folded (`-fold 1`) SFS in
511 realSFS using the SAF file and calculated heterozygosity as the second value (count of
512 heterozygous sites) divided by the total count of analyzed sites. To test for differences in
513 mean individual heterozygosity across time periods, we performed an unequal variances *t*-
514 test comparing all samples within each time category for each of the focal species.

For the three focal species with population-level samples, we estimated nucleotide diversity, Watterson's θ, and Tajima's D per sampled population using thetaStat, included with ANGSD. As the estimates of these metrics, especially Watterson's θ and Tajima's D, can depend on sample size, we made our estimates using 100 subsamples of each population to four individuals. For each subsample, we estimated a SAF file in the same fashion as the heterozygosity estimates, additionally limited to sites for which three of the four subsampled individuals had data (`-minInd 3`). We then used realSFS to generate a folded SFS and thetaStat to estimate these three diversity metrics from the SAF file and SFS in 10kb sliding windows with a step size of 5kb, excluding windows with less than 1000 usable sites. The per site estimate of these three metrics was obtained for each window by dividing the window estimate by the number of usable sites (`nsites`). We report the median estimate across subsamples as the population estimate of each metric. To statistically assess differences between historical and modern populations, we performed a paired difference Wilcoxon signed-rank test on each of the corresponding historical and modern subsamples, pairing estimates by genomic window. We estimated the effect size using the following equation:

$$\frac{Z}{\sqrt{N_{win}}}$$

where Z is the Z-score from the Wilcoxon signed-rank test and N_{win} is the number of paired windows. We considered modern populations to have significantly different estimates of nucleotide diversity, Watterson's θ, or Tajima's D if the distribution of effect sizes across all 100 subsample tests did not overlap 0.

Genetic Differentiation

We estimated genetic differentiation using pairwise population F_{ST} using realSFS. We generated population SAF files using the same parameters as for the genetic diversity metrics and generated a two dimensional folded SFS for each population pair using realSFS. We then used this SFS and the population SAF files to estimate a global estimate of F_{ST} using the Bhatia-Hudson estimator (`-whichFst 1`), which is less sensitive to small or

542 uneven sample sizes (111). Where reported, F_{ST} estimates refer to the weighted F_{ST}. To
543 statistically assess differences in F_{ST} between modern and historical populations, we
544 performed two tests: I) a paired *t*-test pairing corresponding population pairs in historical
545 and modern population sets and II) an unequal variances unpaired *t*-test incorporating all
546 possible population pairs in each set, comparing the historical to the modern population
547 set.

548 *Relatedness*

549 As the analyses we utilize to assess population structure can be sensitive to the presence
550 of close relatives in the dataset, we estimated pairwise relatedness between all samples
551 within each species dataset. We utilized the IBSrelate SFS-based method (112), as
552 implemented in NGSrelate (113), to estimate R0, R1, and KING-robust kinship coefficients
553 (114) for all pairs of individuals in the dataset. For input, we generated a Beagle file using
554 ANGSD for each focal species dataset (`-doGlf 2`), utilizing only positions where greater
555 than 80% of the individuals had data, calling single nucleotide polymorphisms (SNPs) (-
556 `SNP_pval 1e-6`) and assuming known major and minor alleles inferred from the genotype
557 likelihoods (`-doMajorMinor 1 -doMaf 1`) (115, 116).

558 *Population Structure*

559 We explored population structure using principal component analysis (PCA) as
560 implemented in PCAngsd v1.10 (117). As the population structure methods we use
561 assume independence of sites, we first estimated linkage disequilibrium for SNPs less
562 than 50kb apart in the species dataset Beagle files using ngsLD v1.2.0 (118). We pruned
563 SNPs using the recommended prune_graph tool (https://github.com/fgvieira/prune_graph;
564 v0.3.2), assuming independence of SNPs >50kb apart and with a coefficient of correlation
565 (r^2) < 0.1 and subset the Beagle file to include only pruned sites. We then removed one
566 individual from each pair of third-degree or closer relatives in the dataset (expected KING-
567 kinship coefficient >= 0.0625; Table S14) before running the analysis.

568 We formally tested for the presence of population structure using an admixture analysis for
569 1-10 ancestral clusters (K) using the pruned, relative removed Beagle file in NGSadmix v33

570 (119). We performed at least 20 replicate runs for each value of K, up to 100 total runs,
571 stopping if the three highest likelihood replicates converged within 2 log-likelihood units of
572 each other. The 'best-fit' value for K was then determined to be the highest K for which
573 replicates met this convergence criteria, following Pečnerová et al (108). We further
574 assessed the quality of the model fit for each value of K using evalAdmix v0.961 (120).

575 *Genotype Calling*

576 To estimate runs of homozygosity and deleterious burden in our three focal species, we
577 utilized methods that require genotype calls. As deleterious burden estimates can be
578 biased by variation in sequencing depth (19), we subsampled all samples to a mean 5X
579 filtered sequencing depth using Samtools, excluding samples with a mean filtered
580 sequencing depth below 5X from genotype call based analyses. We called genotypes per
581 sample using BCFtools multi-allelic caller v1.19 (100). We called genotypes only for
582 regions in the species-specific filtered sites files, using reads with a minimum mapping
583 quality of 30 and bases with a minimum quality of 20. We set genotypes with a read depth
584 <4 to missing and heterozygous genotypes where one allele was supported by <20% of the
585 reads to missing. We then merged both historical and modern samples into single species-
586 specific BCFs, removing SNPs within 5bp of indels, indels, and including only biallelic
587 SNPs which segregated in the combined historical and modern sample dataset. Finally, we
588 only included sites with called genotypes in 80% of samples and excluded all transition
589 variants.

590 *Runs of Homozygosity*

591 We assessed rates of recent and background inbreeding by estimating the inbreeding
592 coefficient F_{RoH}, the proportion of the autosomal genome existing in runs of homozygosity
593 over a specified length, for each individual from the genotype calls. We incorporated runs
594 of homozygosity >100kb into our estimates of F_{RoH}. We estimated runs of homozygosity
595 using BCFtools/RoH v1.19 (121), setting a constant species-specific recombination rate (-
596 `M`; estimated assuming 50 centimorgans per autosomal chromosome as in Mackintosh et
597 al (26), estimates in Table S12) and running the analysis on genotype calls only, with the PL

598 of unseen genotypes set to 30 (`-G30`). As we did not have sufficient samples to confidently
599 estimate population allele frequencies, we used a default minor allele frequency of 0.4 (`--`
600 `AF-dflt 0.4`). We additionally ignored homozygous reference positions (`--ignore-`
601 `homref`), as including these can inflate estimates of F_{RoH} when using a default allele
602 frequency based on our testing (Figure S9). We calculated F_{RoH} for each individual by
603 dividing the total sum of runs of homozygosity greater than 100kb in length by the total
604 length of the autosomes.

605 *Deleterious mutation burden*

606 We estimated individual levels of deleterious mutation burden from the genotype calls
607 using two complementary methods, one targeting conserved regions of the genome (122)
608 and the other utilizing gene annotations to infer functional effects (123). For these
609 analyses, we utilized the species-specific BCFs, additionally filtering to include only
610 positions with a genotyping rate of 80% in both the historical and the modern sample
611 subsets. As variants were called across the combined historical and modern sample set
612 for each species, alleles that are fixed within one time category, but variable or fixed for the
613 opposing allele in the other, are included.

614 To estimate to which extent the focal species had accumulated putatively deleterious
615 variants in conserved regions of the genome, we used the GenErode pipeline v0.6.0 (124)
616 to estimate Genomic Evolutionary Rate Profiling (GERP) scores (85) across each of the
617 three focal species genomes. The method implemented in this pipeline does not require a
618 multi-species alignment, instead fragmenting the outgroup genomes and mapping the
619 fragments to the target to generate alignments which are then used to estimate scores. We
620 used a dataset of 106 Lepidoptera chromosome-level outgroup genomes (Table S15) to
621 estimate the scores and ancestral states, using divergence times estimated with TimeTree
622 5 (125). We selected the top 1% of GERP scores as the most conserved positions using the
623 `get_gerp_score_percentile.py` script included with GenErode. For each individual, we
624 estimated deleterious burden at conserved positions using a GERP-scaled relative count
625 of derived alleles at the top conserved positions, considering the derived allele to be

putatively deleterious. Total deleterious burden at conserved positions for each individual was calculated by summing the multiple of the derived allele count and GERP score at each conserved position, scaled per 1000 derived alleles. We estimated homozygous deleterious burden by calculating the same relative count, but only including homozygous derived genotypes.

For the functional annotation based method, we used the genome annotations provided by the Darwin Tree of Life Project (https://projects.ensembl.org/darwin-tree-of-life/). We assigned impacts to each variant using Ensembl's Variant Effect Predictor (VEP) v112.0 (123). VEP categorizes variants into four classes: 'High', 'Moderate', 'Low', or 'Modifier', which largely correspond to loss of function, missense, synonymous, and intergenic variants. As variants often overlap multiple transcripts, multiple impacts will be assigned, so we required VEP to pick one effect per variant (`--flag_pick`), using the default selection order (123). For each individual, we estimated deleterious burden from strongly (including variants classified as 'High' impact, e.g. loss of function) and weakly (including variants classified as 'Moderate' impact, i.e. missense) deleterious variants using a relative count of alternate alleles at these positions, which we treated as the putatively deleterious alleles. Total deleterious burden for each individual is the count of alternate alleles for the variant category of interest per 1000 alternate alleles. Homozygous deleterious burden is the count of alternate alleles at homozygous positions for the variant category of interest per 1000 alternate alleles.

Categorizing rates of genetic decline

To assess the changes in genetic diversity in a framework developed for conservation focused genetic monitoring, we used the indicator thresholds suggested by Andersson et al (20), which are based upon indicators applied for national use in Sweden (126). Using these thresholds, genetic decline within populations is measured as the amount of genetic diversity retained over a period of 100 years, assuming a constant rate of change. Three threat categories are suggested: retention >=95% is considered 'Acceptable', 75-94% as 'Warning', and <75% as 'Alarm'. As different population genetic estimates of genetic

654 diversity are influenced by different components of genetic diversity, such as rare and
655 common variants, this metric can be assessed for each estimate separately.

656 We estimated the predicted retention of genetic diversity over 100 years for each
657 population using individual heterozygosity, nucleotide diversity, and Watterson's θ.
658 Genetic diversity retention per year was estimated using the following equation:

659 $$e^{\frac{ln(H_{mod}/H_{hist})}{Y_{mod}-Y_{hist}}}$$

660 where H is the estimate of genetic diversity for a given sample/population and Y is the
661 sampling year for that sample/population. As different populations had different sample
662 sizes, we used repeated subsamples to generate estimates of decline. For individual
663 heterozygosity, we performed all pairwise comparisons of historical and modern individual
664 estimates of heterozygosity within corresponding historical-modern sample pairs,
665 generating a single estimate for species with only one specimen per time period and a
666 range for ones with more (see Figure 4). For nucleotide diversity and Watterson's θ, we
667 utilized the previously generated 100 subsamples (N=4) for each population, estimating
668 H_{mod}/H_{hist} for paired historical and modern populations for each subsample, utilizing the
669 median value of H_{mod}/H_{hist} across subsamples to calculate the predicted retention.

670 Acknowledgements

671 We would like to thank Melina Eberhagen, Amanda Görnerup, Kajsa Svensson, Aske
672 Brydegaard Runemark, and Mikkel Brydegaard for assistance with collecting butterflies,
673 Håkan Elmqvist for providing pinned specimens of *Ph. alcon* and *S. orion*, Göran Engqvist
674 for providing tissue from the pinned specimen of *Pl. argyrognomon*, Emma Kärrnäs and
675 Isolde van Riemsdijk for assistance with DNA extractions, Jadranka Rota for assistance
676 with the entomological collections of the Biological Museum, Lund University
677 (https://doi.org/10.15468/dahk2a), Verena Kutschera and the Swedish Bioinformatics
678 Advisory Program for advice regarding the bioinformatic analyses, Anna Penna for
679 comments on the manuscript, and Isolde van Riemsdijk, Rachel Steward, Kalle Tunström,
680 Simon Jacobsen Ellestrand, Colin Olito, and Magne Friberg for helpful discussions

regarding the study species, methods and interpretations. We acknowledge support from the National Genomics Infrastructure in Genomics Production Stockholm funded by Science for Life Laboratory, the Knut and Alice Wallenberg Foundation and the Swedish Research Council. The computations were enabled by resources provided by the National Academic Infrastructure for Supercomputing in Sweden (NAISS) and the Swedish National Infrastructure for Computing (SNIC) at UPPMAX partially funded by the Swedish Research Council through grant agreements no. 2022-06725 and no. 2018-05973. This work was supported by grants from the Strategic Research Area "Biodiversity and Ecosystem services in a Changing Climate" (BECC), funded by the Swedish government, the Foundation Oscar och Lili Lamms Minne, the Jörgen Lindström's Foundation, and the Swedish Research Council for Sustainable Development (grant 2021-01163).

Data Availability Statement

The genetic data that support these findings will be made available upon publication at NCBI in BioProjects PRJNA1068054 (focal species, modern) & PRJNA1168917 (focal species, historical; additional species). The main population genomic pipeline is deposited at https://doi.org/10.5281/zenodo.13785563. Workflow configurations, extensions, and resources specific to this study are archived at https://doi.org/10.5281/zenodo.13902816.

References

1. D. L. Wagner, E. M. Grames, M. L. Forister, M. R. Berenbaum, D. Stopak, Insect decline in the anthropocene: Death by a thousand cuts. *Proceedings of the National Academy of Sciences* **118**, e2023989118 (2021).

2. R. van Klink, *et al.*, Meta-analysis reveals declines in terrestrial but increases in freshwater insect abundances. *Science* **368**, 417–420 (2020).

3. R. Dirzo, *et al.*, Defaunation in the Anthropocene. *Science* **345**, 401–406 (2014).

4. C. A. Halsch, *et al.*, Insects and recent climate change. *Proceedings of the National Academy of Sciences* **118**, e2002543117 (2021).

5. P. H. Raven, D. L. Wagner, Agricultural intensification and climate change are rapidly decreasing insect biodiversity. *Proceedings of the National Academy of Sciences* **118**, e2002548117 (2021).

6. S. Seibold, *et al.*, Arthropod decline in grasslands and forests is associated with landscape-level drivers. *Nature* **574**, 671–674 (2019).

7. D. H. Boyes, D. M. Evans, R. Fox, M. S. Parsons, M. J. O. Pocock, Is light pollution driving moth population declines? A review of causal mechanisms across the life cycle. *Insect Conservation and Diversity* **14**, 167–187 (2021).

8. J. R. Shipley, *et al.*, Agricultural practices and biodiversity: Conservation policies for semi-natural grasslands in europe. *Current Biology* **34**, R753–R761 (2024).

9. R. C. Lacy, Loss of Genetic Diversity from Managed Populations: Interacting Effects of Drift, Mutation, Immigration, Selection, and Population Subdivision. *Conservation Biology* **1**, 143–158 (1987).

10. R. Lande, Mutation and Conservation. *Conservation Biology* **9**, 782–791 (1995).

11. R. Lande, S. Shannon, The Role of Genetic Variation in Adaptation and Population Persistence in a Changing Environment. *Evolution* **50**, 434–437 (1996).

12. G. Bertorelle, *et al.*, Genetic load: genomic estimates and applications in non-model animals. *Nature Reviews Genetics* **23**, 492–503 (2022).

13. M. Lynch, J. Conery, R. Burger, Mutation accumulation and the extinction of small populations. *The American Naturalist* **146**, 489–518 (1995).

14. J. F. Crow, Some possibilities for measuring selection intensities in man. *Human Biology* **30**, 1–13 (1958).

15. M. Lynch, W. Gabriel, Mutation Load and the Survival of Small Populations. *Evolution* **44**, 1725–1737 (1990).

16. D. L. Gilroy, K. P. Phillips, D. S. Richardson, C. van Oosterhout, Toll-like receptor variation in the bottlenecked population of the Seychelles warbler: computer simulations see the 'ghost of selection past' and quantify the 'drift debt'. *Journal of Evolutionary Biology* **30**, 1276–1287 (2017).

17. A. V. Pinto, B. Hansson, I. Patramanis, H. E. Morales, C. van Oosterhout, The impact of habitat loss and population fragmentation on genomic erosion. *Conservation Genetics* **25**, 49–57 (2024).

18. H. A. Jackson, *et al.*, Genomic erosion in a demographically recovered bird species during conservation rescue. *Conservation Biology* **36**, e13918 (2022).

19. M. Dehasque, *et al.*, Temporal dynamics of woolly mammoth genome erosion prior to extinction. *Cell* **187**, 3531–3540.e13 (2024).

20. A. Andersson, S. Karlsson, N. Ryman, L. Laikre, Monitoring genetic diversity with new indicators applied to an alpine freshwater top predator. *Molecular Ecology* **31**, 6422–6439 (2022).

21. D. O'Brien, *et al.*, Bringing together approaches to reporting on within species genetic diversity. *Journal of Applied Ecology* **59**, 2227–2233 (2022).

22. K. Theissinger, *et al.*, How genomics can help biodiversity conservation. *Trends in Genetics* **39**, 545–559 (2023).

23. D. Díez-del-Molino, F. Sánchez-Barreiro, I. Barnes, M. T. P. Gilbert, L. Dalén, Quantifying temporal genomic erosion in endangered species. *Trends in Ecology & Evolution* **33**, 176–185 (2018).

24. H. Ellegren, N. Galtier, Determinants of genetic diversity. *Nature Reviews Genetics* **17**, 422–433 (2016).

25. J. Romiguier, *et al.*, Comparative population genomics in animals uncovers the determinants of genetic diversity. *Nature* **515**, 261–263 (2014).

26. A. Mackintosh, *et al.*, The determinants of genetic diversity in butterflies. *Nature Communications* **10**, 3466 (2019).

27. G. Hewitt, The genetic legacy of the Quaternary ice ages. *Nature* **405**, 907–913 (2000).

28. J. A. Robinson, *et al.*, Genomic flatlining in the endangered island fox. *Current Biology* **26**, 1183–1189 (2016).

29. J. A. Robinson, *et al.*, The critically endangered vaquita is not doomed to extinction by inbreeding depression. *Science* **376**, 635–639 (2022).

30. M. F. DiLeo, A. Nair, M. Kardos, A. Husby, M. Saastamoinen, Demography and environment modulate the effects of genetic diversity on extinction risk in a butterfly metapopulation. *Proceedings of the National Academy of Sciences* **121**, e2309455121 (2024).

31. J. C. Teixeira, C. D. Huber, The inflated significance of neutral genetic diversity in conservation genetics. *Proceedings of the National Academy of Sciences* **118**, e2015096118 (2021).

32. A. García-Dorado, A. Caballero, Neutral genetic diversity as a useful tool for conservation biology. *Conservation Genetics* **22**, 541–545 (2021).

33. M. Kardos, H. R. Taylor, H. Ellegren, G. Luikart, F. W. Allendorf, Genomics advances the study of inbreeding depression in the wild. *Evolutionary Applications* **9**, 1205–1218 (2016).

34. M. K. Schwartz, G. Luikart, R. S. Waples, Genetic monitoring as a promising tool for conservation and management. *Trends in Ecology & Evolution* **22**, 25–33 (2007).

35. S. Hoban, *et al.*, Effective population size remains a suitable, pragmatic indicator of genetic diversity for all species, including forest trees. *Biological Conservation* **253**, 108906 (2021).

36. M. Kardos, *et al.*, The crucial role of genome-wide genetic variation in conservation. *Proceedings of the National Academy of Sciences* **118**, e2104642118 (2021).

37. N. Dussex, H. E. Morales, C. Grossen, L. Dalén, C. van Oosterhout, Purging and accumulation of genetic load in conservation. *Trends in Ecology & Evolution* **38**, 961–969 (2023).

38. C. van Oosterhout, Mutation load is the spectre of species conservation. *Nature Ecology & Evolution* **4**, 1004–1006 (2020).

39. T. van der Valk, D. Díez-del-Molino, T. Marques-Bonet, K. Guschanski, L. Dalén, Historical Genomes Reveal the Genomic Consequences of Recent Population Decline in Eastern Gorillas. *Current Biology* **29**, 165–170.e6 (2019).

40. J. von Seth, *et al.*, Genomic insights into the conservation status of the world's last remaining Sumatran rhinoceros populations. *Nature Communications* **12**, 2393 (2021).

41. G. Femerling, *et al.*, Genetic Load and Adaptive Potential of a Recovered Avian Species that Narrowly Avoided Extinction. *Molecular Biology and Evolution* **40**, msad256 (2023).

42. M. Ihse, Swedish agricultural landscapes patterns and changes during the last 50 years, studied by aerial photos. *Landscape and Urban Planning* **31**, 21–37 (1995).

43. R. Lindborg, O. Eriksson, Historical Landscape Connectivity Affects Present Plant Species Diversity. *Ecology* **85**, 1840–1845 (2004).

44. D. L. Wagner, R. Fox, D. M. Salcido, L. A. Dyer, A window to the world of global insect declines: Moth biodiversity trends are complex and heterogeneous. *Proceedings of the National Academy of Sciences* **118**, e2002549117 (2021).

45. M. S. Warren, *et al.*, The decline of butterflies in europe: Problems, significance, and possible solutions. *Proceedings of the National Academy of Sciences* **118**, e2002551117 (2021).

46. J. C. Habel, *et al.*, Butterfly community shifts over two centuries. *Conservation Biology* **30**, 754–762 (2016).

47. SLU Artdatabanken, *Rödlistade arter i Sverige 2020* (SLU, 2020).

48. C. Fägerström, Lund University Biological Museum - Insect collections Inventory. (2024). https://doi.org/10.15468/dahk2a.

49. Z. J. Nolen, M. Rundlöf, A. Runemark, Species-specific erosion of genetic diversity in grassland butterflies depends on landscape land cover. *Biological Conservation* **296**, 110694 (2024).

50. M. T. P. Gilbert, *et al.*, Recharacterization of ancient DNA miscoding lesions: Insights in the era of sequencing-by-synthesis. *Nucleic Acids Research* **35**, 1–10 (2007).

51. M. Stiller, *et al.*, Patterns of nucleotide misincorporations during enzymatic amplification and direct large-scale sequencing of ancient DNA. *Proceedings of the National Academy of Sciences* **103**, 13578–13584 (2006).

52. H. Jónsson, A. Ginolhac, M. Schubert, P. L. F. Johnson, L. Orlando, mapDamage2.0: Fast approximate bayesian estimates of ancient DNA damage parameters. *Bioinformatics* **29**, 1682–1684 (2013).

53. P. W. Hedrick, *Genetics of Populations* (Jones & Bartlett Publishers, 2009).

54. R. McQuillan, *et al.*, Runs of homozygosity in european populations. *The American Journal of Human Genetics* **83**, 359–372 (2008).

55. E. A. Thompson, Identity by descent: Variation in meiosis, across genomes, and in populations. *Genetics* **194**, 301–326 (2013).

56. S. Glémin, How are deleterious mutations purged? Drift versus nonrandom mating. *Evolution* **57**, 2678–2687 (2003).

57. M. Kirkpatrick, P. Jarne, The effects of a bottleneck on inbreeding depression and the genetic load. *The American Naturalist* **155**, 154–167 (2000).

58. J. Wang, W. G. Hill, D. Charlesworth, B. Charlesworth, Dynamics of inbreeding depression due to deleterious mutations in small populations: mutation parameters and inbreeding rate. *Genetics Research* **74**, 165–178 (1999).

59. B. Charlesworth, Mutational load, inbreeding depression and heterosis in subdivided populations. *Molecular Ecology* **27**, 4991–5003 (2018).

60. D. Kleinman-Ruiz, *et al.*, Purging of deleterious burden in the endangered iberian lynx. *Proceedings of the National Academy of Sciences* **119**, e2110614119 (2022).

61. E. Humble, *et al.*, Conservation management strategy impacts inbreeding and mutation load in scimitar-horned oryx. *Proceedings of the National Academy of Sciences* **120**, e2210756120 (2023).

62. SLU Artdatabanken, Artfakta: kronärtsblåvinge (Plebejus argyrognomon).

63. J. C. Habel, M. J. Samways, T. Schmitt, Mitigating the precipitous decline of terrestrial European insects: Requirements for a new strategy. *Biodiversity and Conservation* **28**, 1343–1360 (2019).

64. E. L. Landguth, *et al.*, Quantifying the lag time to detect barriers in landscape genetics. *Molecular Ecology* **19**, 4179–4191 (2010).

65. C. W. Epps, N. Keyghobadi, Landscape genetics in a changing world: disentangling historical and contemporary influences and inferring change. *Molecular Ecology* **24**, 6021–6040 (2015).

66. W. H. Lowe, F. W. Allendorf, What can genetics tell us about population connectivity? *Molecular Ecology* **19**, 3038–3051 (2010).

67. P. W. Hedrick, J. R. Adams, J. A. Vucetich, Reevaluating and Broadening the Definition of Genetic Rescue. *Conservation Biology* **25**, 1069–1070 (2011).

68. P. W. Hedrick, A. Garcia-Dorado, Understanding inbreeding depression, purging, and genetic rescue. *Trends in Ecology & Evolution* **31**, 940–952 (2016).

69. D. A. Bell, *et al.*, The Exciting Potential and Remaining Uncertainties of Genetic Rescue. *Trends in Ecology & Evolution* **34**, 1070–1079 (2019).

70. R. Lande, Risk of population extinction from fixation of new deleterious mutations. *Evolution* **48**, 1460–1469 (1994).

71. Y. B. Simons, G. Sella, The impact of recent population history on the deleterious mutation load in humans and close evolutionary relatives. *Current Opinion in Genetics & Development* **41**, 150–158 (2016).

72. Y. Xue, *et al.*, Mountain gorilla genomes reveal the impact of long-term population decline and inbreeding. *Science* **348**, 242–245 (2015).

73. C. Grossen, F. Guillaume, L. F. Keller, D. Croll, Purging of highly deleterious mutations through severe bottlenecks in Alpine ibex. *Nature Communications* **11**, 1001 (2020).

74. N. Dussex, *et al.*, Population genomics of the critically endangered kākāpō. *Cell Genomics* **1**, 100002 (2021).

75. A. Khan, *et al.*, Genomic evidence for inbreeding depression and purging of deleterious genetic variation in indian tigers. *Proceedings of the National Academy of Sciences* **118**, e2023018118 (2021).

76. B. Charlesworth, Evidence against Fisher's theory of dominance. *Nature* **278**, 848–849 (1979).

77. F. Manna, G. Martin, T. Lenormand, Fitness landscapes: An alternative theory for the dominance of mutation. *Genetics* **189**, 923–937 (2011).

78. A. García-Dorado, A. Caballero, On the average coefficient of dominance of deleterious spontaneous mutations. *Genetics* **155**, 1991–2001 (2000).

79. C. D. Huber, A. Durvasula, A. M. Hancock, K. E. Lohmueller, Gene expression drives the evolution of dominance. *Nature Communications* **9**, 2750 (2018).

80. B. Charlesworth, D. Charlesworth, *Elements of evolutionary genetics* (Roberts; Company, 2010).

81. L. F. Keller, D. M. Waller, Inbreeding effects in wild populations. *Trends in Ecology & Evolution* **17**, 230–241 (2002).

82. D. Charlesworth, J. H. Willis, The genetics of inbreeding depression. *Nature Reviews Genetics* **10**, 783–796 (2009).

83. A. L. K. Mattila, *et al.*, High genetic load in an old isolated butterfly population. *Proceedings of the National Academy of Sciences* **109**, E2496–E2505 (2012).

84. I. Saccheri, *et al.*, Inbreeding and extinction in a butterfly metapopulation. *Nature* **392**, 491–494 (1998).

85. G. M. Cooper, *et al.*, Distribution and intensity of constraint in mammalian genomic sequence. *Genome Research* **15**, 901–913 (2005).

86. C. D. Huber, B. Y. Kim, K. E. Lohmueller, Population genetic models of GERP scores suggest pervasive turnover of constrained sites across mammalian evolution. *PLOS Genetics* **16**, e1008827 (2020).

87. C. C. Kyriazis, J. A. Robinson, K. E. Lohmueller, Using computational simulations to model deleterious variation and genetic load in natural populations. *The American Naturalist* **202**, 737–752 (2023).

900 88. C. Bortoluzzi, *et al.*, Lepidoptera genomics based on 88 chromosomal reference
901 sequences informs population genetic parameters for conservation. *bioRxiv* (2023).
902 https://doi.org/10.1101/2023.04.14.536868.

903 89. L. B. Pettersson, H. Arnberg, *Svensk dagfjärilsövervakning, årsrapport för 2023*
904 (Biologiska institutionen, Lunds universitet, 2024).

905 90. S. Hoban, *et al.*, Genetic diversity targets and indicators in the CBD post-2020
906 Global Biodiversity Framework must be improved. *Biological Conservation* **248**, 108654
907 (2020).

908 91. L. Laikre, *et al.*, Post-2020 goals overlook genetic diversity. *Science* **367**, 1083–1085
909 (2020).

910 92. G. Formenti, *et al.*, The era of reference genomes in conservation genomics. *Trends*
911 *in Ecology & Evolution* **37**, 197–202 (2022).

912 93. V. G. Twort, J. Minet, C. W. Wheat, N. Wahlberg, Museomics of a rare taxon: placing
913 Whalleyanidae in the Lepidoptera Tree of Life. *Systematic Entomology* **46**, 926–937 (2021).

914 94. Z. J. Nolen, Zjnolen/PopGLen: V0.3.0. (2024).
915 https://doi.org/10.5281/zenodo.13785563. Deposited September 2024.

916 95. F. Mölder, *et al.*, Sustainable data analysis with snakemake [version 2; peer review:
917 2 approved]. *F1000Research* **10** (2021).

918 96. S. Chen, Y. Zhou, Y. Chen, J. Gu, Fastp: An ultra-fast all-in-one FASTQ preprocessor.
919 *Bioinformatics* **34**, i884–i890 (2018).

920 97. H. Li, Aligning sequence reads, clone sequences and assembly contigs with BWA-
921 MEM. (2013). https://doi.org/10.48550/arXiv.1303.3997.

922 98. H. Li, R. Durbin, Fast and accurate long-read alignment with BurrowsWheeler
923 transform. *Bioinformatics* **26**, 589–595 (2010).

924 99. E. Palkopoulou, *et al.*, Complete genomes reveal signatures of demographic and
925 genetic declines in the woolly mammoth. *Current biology: CB* **25**, 1395–1400 (2015).

926 100. P. Danecek, *et al.*, Twelve years of SAMtools and BCFtools. *GigaScience* **10** (2021).

927 101. Picard toolkit. *Broad Institute, GitHub Repository* (2019). Deposited 2019.

928 102. A. Peltzer, *et al.*, EAGER: efficient ancient genome reconstruction. *Genome Biology*
929 **17**, 1–14 (2016).

930 103. G. A. van der Auwera, B. D. O'Connor, *Genomics in the Cloud: Using Docker, GATK,*
931 *and WDL in Terra* (O'Reilly Media, Inc., 2020).

932 104. T. S. Korneliussen, A. Albrechtsen, R. Nielsen, ANGSD: Analysis of Next Generation
933 Sequencing Data. *BMC Bioinformatics* **15**, 1–13 (2014).

934 105. R. N. Lou, A. Jacobs, A. P. Wilder, N. O. Therkildsen, A beginner's guide to low-
935 coverage whole genome sequencing for population genomics. *Molecular Ecology* **30**,
936 5966–5993 (2021).

937 106. G. Jun, M. K. Wing, G. R. Abecasis, H. M. Kang, An efficient and scalable analysis
938 framework for variant extraction and refinement from population-scale DNA sequence
939 data. *Genome Research* **25**, 918–925 (2015).

940 107. J. Neukamm, A. Peltzer, K. Nieselt, DamageProfiler: Fast damage pattern
941 calculation for ancient DNA. *Bioinformatics* **37**, 3652–3653 (2021).

942 108. P. Pečnerová, *et al.*, High genetic diversity and low differentiation reflect the
943 ecological versatility of the African leopard. *Current Biology* **31**, 1862–1871.e5 (2021).

944 109. A. F. A. Smit, R. Hubley, P. Green, RepeatMasker open-4.0. (2013). Deposited 2013.

945 110. S. Gopalakrishnan, *et al.*, The population genomic legacy of the second plague
946 pandemic. *Current Biology* **32**, 4743–4751.e6 (2022).

947 111. G. Bhatia, N. Patterson, S. Sankararaman, A. L. Price, Estimating and interpreting
948 FST: The impact of rare variants. *Genome Research* **23**, 1514–1521 (2013).

949 112. R. K. Waples, A. Albrechtsen, I. Moltke, Allele frequency-free inference of close
950 familial relationships from genotypes or low-depth sequencing data. *Molecular Ecology* **28**,
951 35–48 (2019).

952 113. K. Hanghøj, I. Moltke, P. A. Andersen, A. Manica, T. S. Korneliussen, Fast and
953 accurate relatedness estimation from high-throughput sequencing data in the presence of
954 inbreeding. *GigaScience* **8**, giz034 (2019).

955 114. A. Manichaikul, *et al.*, Robust relationship inference in genome-wide association
956 studies. *Bioinformatics* **26**, 2867–2873 (2010).

957 115. L. Skotte, T. S. Korneliussen, A. Albrechtsen, Association testing for next-generation
958 sequencing data using score statistics. *Genetic Epidemiology* **36**, 430437 (2012).

959 116. S. Y. Kim, *et al.*, Estimation of allele frequency and association mapping using next-
960 generation sequencing data. *BMC Bioinformatics* **12**, 231 (2011).

961 117. J. Meisner, A. Albrechtsen, Inferring population structure and admixture proportions
962 in low-depth NGS data. *Genetics* **210**, 719–731 (2018).

963 118. E. A. Fox, A. E. Wright, M. Fumagalli, F. G. Vieira, ngsLD: Evaluating linkage
964 disequilibrium using genotype likelihoods. *Bioinformatics* **35**, 3855–3856 (2019).

965 119. L. Skotte, T. S. Korneliussen, A. Albrechtsen, Estimating individual admixture
966 proportions from next generation sequencing data. *Genetics* **195**, 693–702 (2013).

967 120. G. Garcia-Erill, A. Albrechtsen, Evaluation of model fit of inferred admixture
968 proportions. *Molecular Ecology Resources* **20**, 936–949 (2020).

969 121. V. Narasimhan, *et al.*, BCFtools/RoH: A hidden markov model approach for
970 detecting autozygosity from next-generation sequencing data. *Bioinformatics* **32**, 1749–
971 1751 (2016).

972 122. E. V. Davydov, *et al.*, Identifying a High Fraction of the Human Genome to be under
973 Selective Constraint Using GERP++. *PLOS Computational Biology* **6**, e1001025 (2010).

974 123. W. McLaren, *et al.*, The Ensembl Variant Effect Predictor. *Genome Biology* **17**, 122
975 (2016).

976 124. V. E. Kutschera, *et al.*, GenErode: a bioinformatics pipeline to investigate genome
977 erosion in endangered and extinct species. *BMC Bioinformatics* **23**, 1–17 (2022).

978 125. S. Kumar, *et al.*, TimeTree 5: An expanded resource for species divergence times.
979 *Molecular Biology and Evolution* **39**, msac174 (2022).

980 126. K. Johannesson, L. Laikre, Monitoring of genetic diversity in environmental
981 monitoring [in Swedish]. *Report to the Swedish Agency for Marine and Water Management*
982 *(dnr. HaV 3642-2018, 3643-2018)* (2020).

983

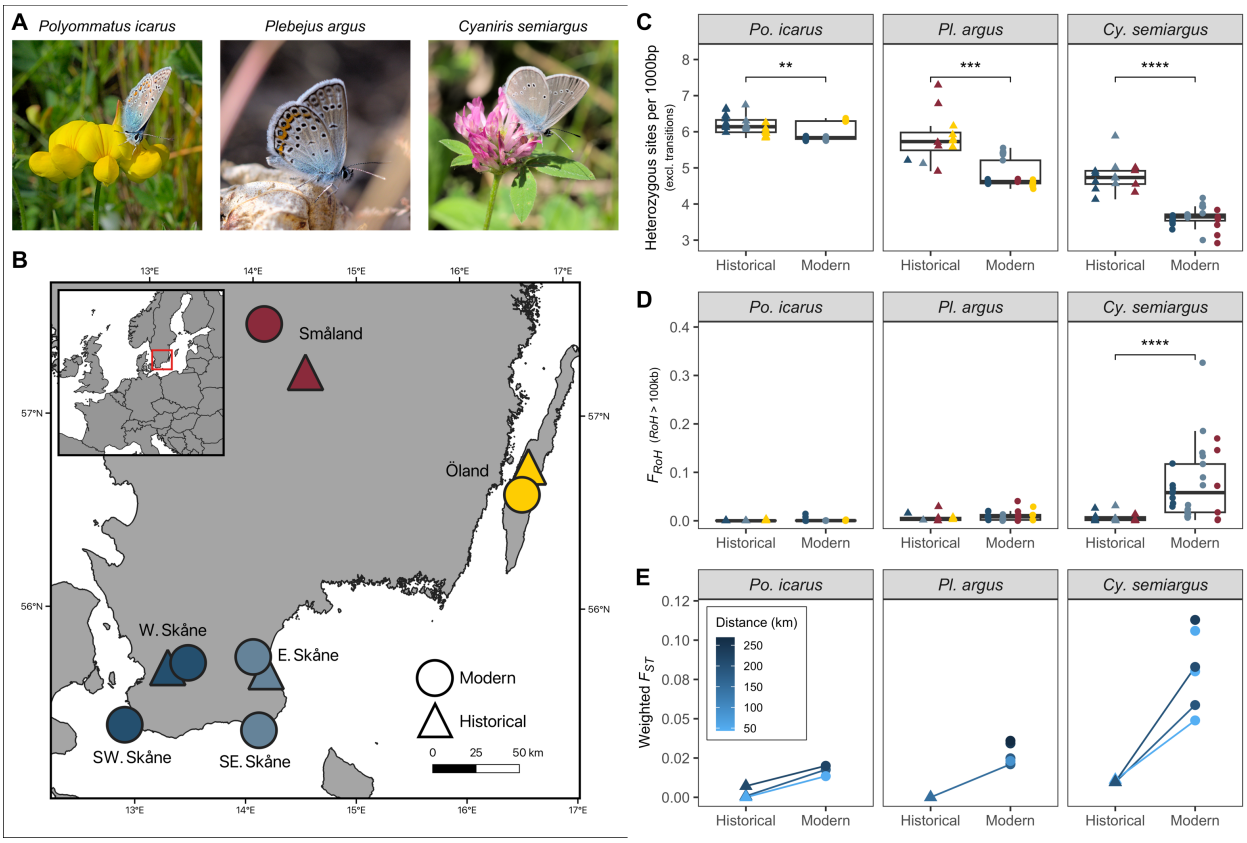

Figure 1: ***Sampling design and changes in genetic diversity, differentiation, and inbreeding in the focal species.*** *(A) Images of the three focal species. (B) Map of the sampling area in southern Sweden, sampling locations are approximate. Circles represent areas with modern samples in at least one of the species and triangles represent areas with historical samples, see Table S1 for complete sampling information. (C) Change in individual heterozygosity over time, measured as heterozygous sites per 1000bp, excluding transitions. Each point represents an individual sample, grouped into historical and modern samples per species. Coloring refers to sampling region and corresponds to the map in panel B. (D) Change in inbreeding coefficients over time, estimated using runs of homozygosity larger than 100kb (F_{RoH}). (E) Change in pairwise population genetic differentiation, F_{ST} over time between equivalent comparisons in each time period. Color of the points and line refer to the geographic distance between populations. Populations with no connecting line refer to pairs of modern sample populations that have no comparable historic pair. In C & D, results of unequal variance t-tests between historical and modern samples for each species is shown using the following scale, where panels without * are not significant (P > 0.05): * P <= 0.05, ** P <= 0.01, *** P <= 0.001, **** P <= 0.0001. Statistical assessment of genetic differentiation is not shown, as it could not be assessed for all three species (Table S7).*

984

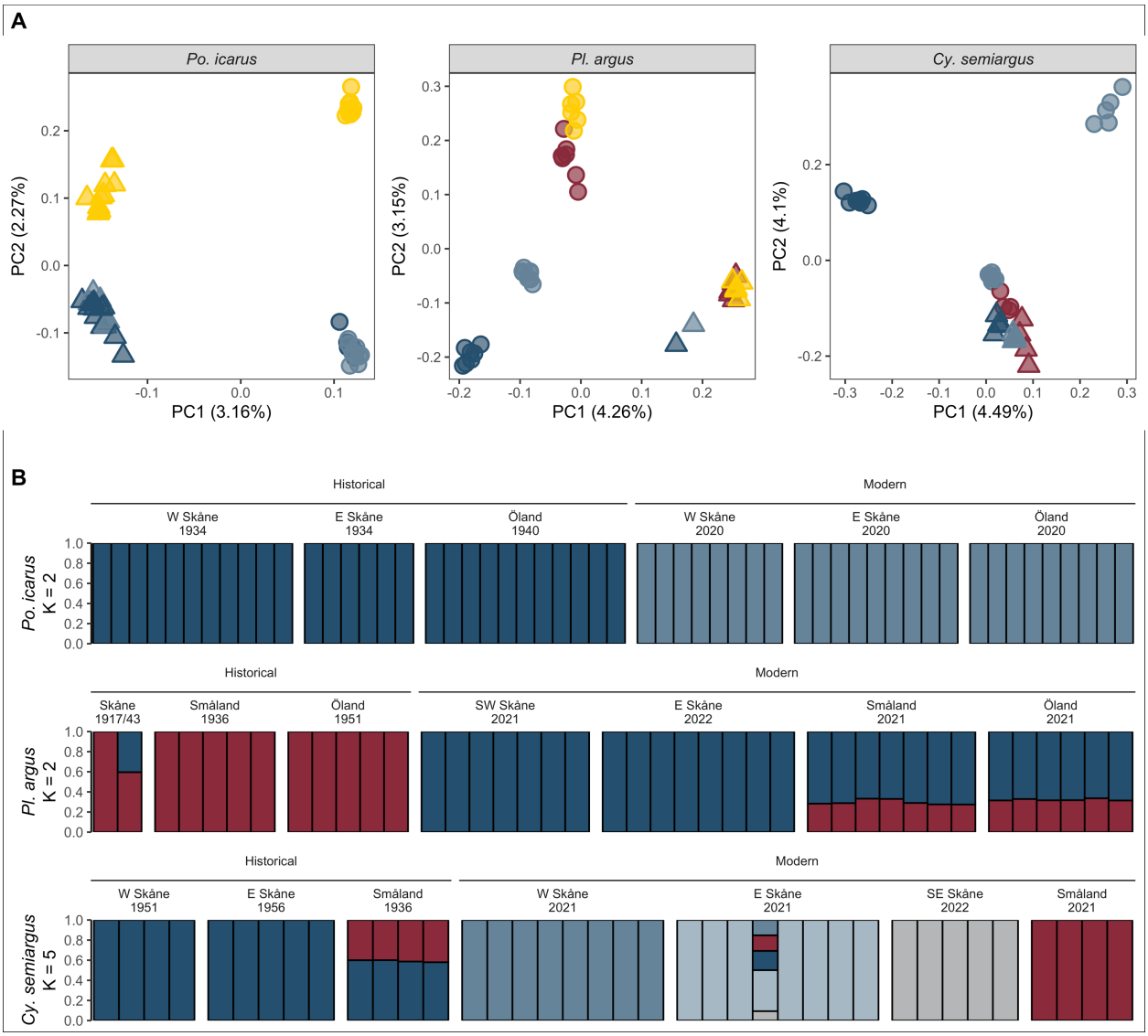

Figure 2: ***Population structure of the focal species.*** *(A) Principal Component Analysis (PCA) of the three focal species. Shapes refer to sampling period, with each circle representing a modern and each triangle a historical individual, with colors corresponding to the sampling locations in Figure 1B. Percentages on each axis refer to the proportion of total variance explained by the component. (B) Best fit admixture analyses for the three focal species. Each bar represents an individual and each color one of K genetic clusters. Each bar is colored in proportion to the probability of the individual belonging to each cluster.*

985

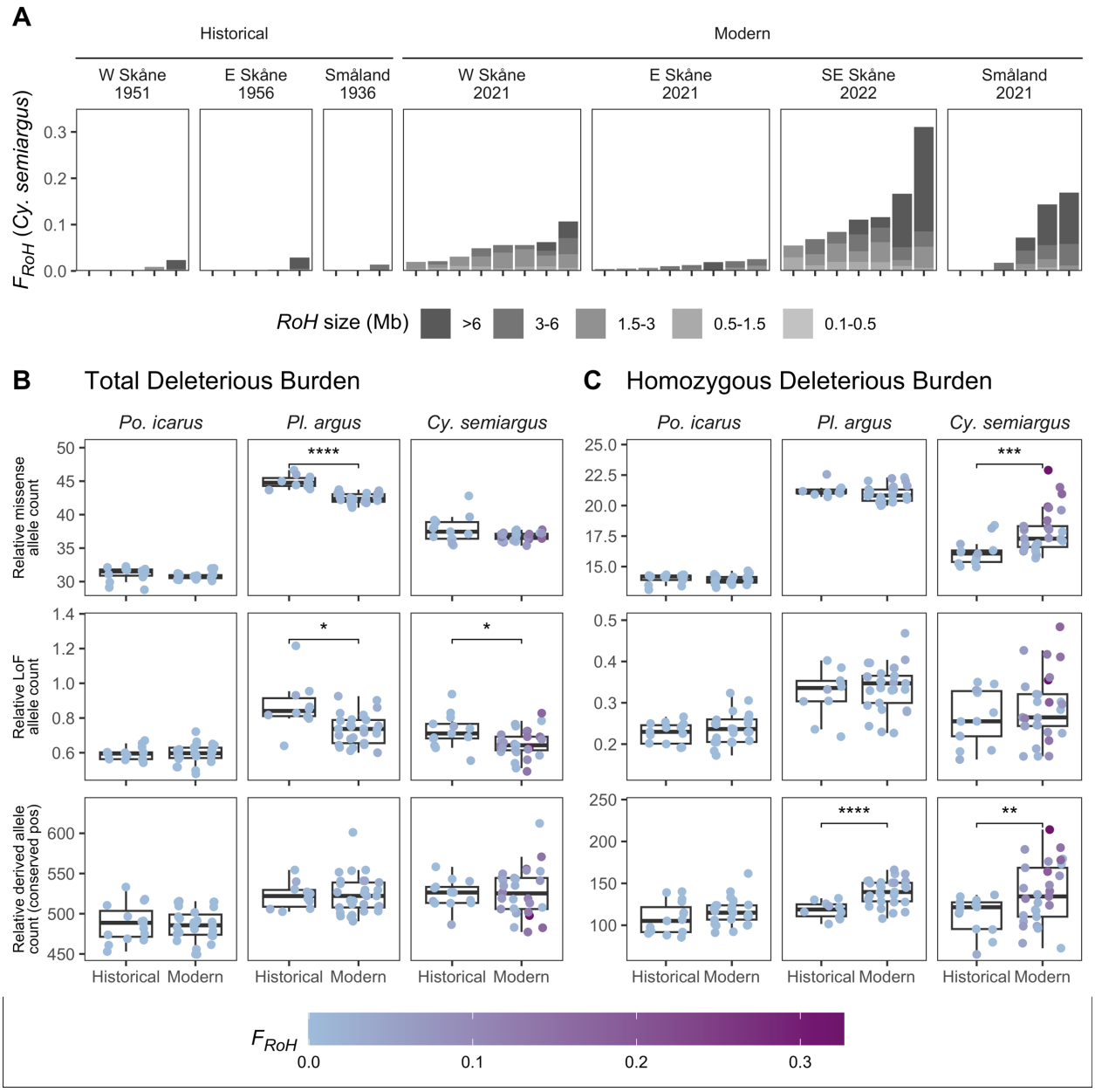

Figure 3: ***Temporal changes in deleterious burden in the focal species*** *(A) Individual inbreeding coefficients (F_{RoH}) partitioned by RoH size class. Longer RoH indicate more recent common ancestry of the identical haplotypes. (B) Estimates of total deleterious mutation burden for each individual of the three focal species across three categories of putatively deleterious mutations: I) missense (i.e. weakly deleterious; upper), II) loss of function (i.e. strongly deleterious; middle), and III) derived mutations in highly conserved regions (lower). Total burden for missense and LoF mutations is the total count of alternate alleles for the given mutation category per 1000 alternate alleles. Total burden for derived mutations at conserved positions is the total count of derived alleles at the top 1% most genomically conserved positions multiplied by their GERP scores, per 1000 derived alleles.*

*C) Homozygous deleterious mutation burden for the same mutation categories as in B, but only calculated using positions homozygous for the putatively deleterious alleles. In B & C, results of unequal variance t-tests comparing deleterious burden between historical and modern samples are shown in each panel, where panels without * are not significant (P > 0.05): * P <= 0.05, ** P <= 0.01, *** P <= 0.001, **** P <= 0.0001.*

986

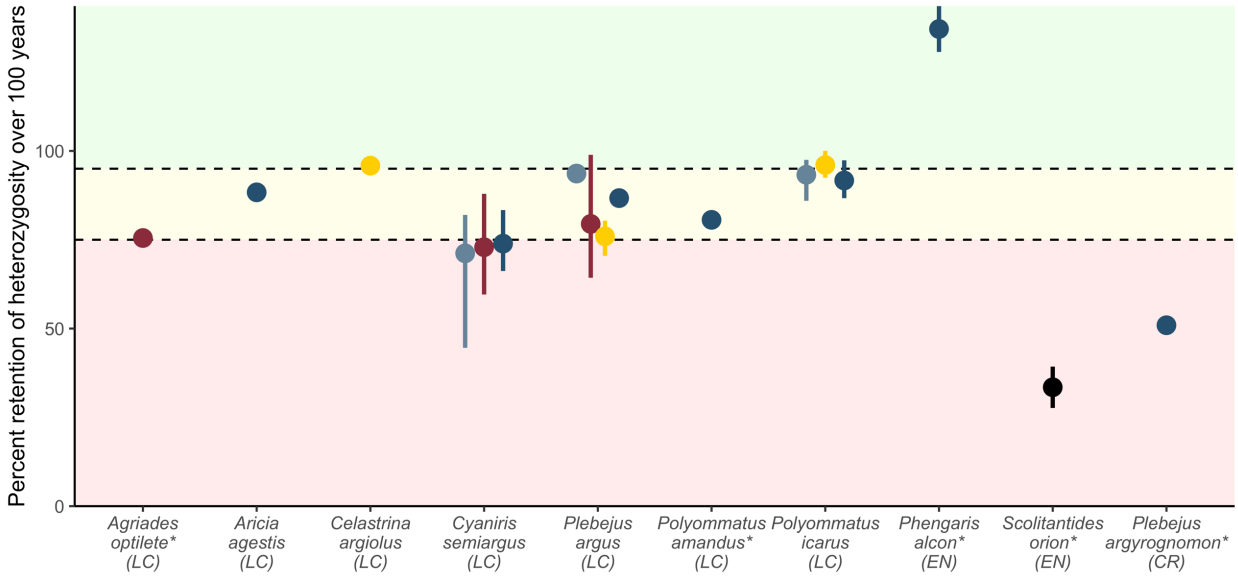

*Figure 4: Changes in heterozygosity predicted over 100 years based on the rate of change estimated from modern and historical samples for each of 11 species. Species are grouped by conservation status, which follows the species name on the x-axis. Background coloration refers to the three genetic decline thresholds outlined by Andersson et al (20), where a retention of >=95% over 100 year is considered 'acceptable' (green), a retention of 75-94% as 'warning' (yellow), and a retention of <75% as 'alarm' (red). Points represent mean estimates for change in heterozygosity across all sample pairs for a species. Species with bars have more than one possible sample pair, with error bars illustrating the spread of estimates across all sample pairs. Species with a * next to their species name on the x-axis have been mapped to a related species' reference genome as they lack a species-specific reference (Table S12).*

987